Evidence for directed percolation universality at the onset of spatiotemporal intermittency in coupled circle maps

T. M. Janaki,[1,*] Sudeshna Sinha,[1,†] and Neelima Gupte[2,‡]
[1]*Institute of Mathematical Sciences, Taramani, Chennai 600 113, India*
[2]*Department of Physics, IIT Madras, Chennai 600036, India*
(Received 14 October 2002; revised manuscript received 17 March 2003; published 27 May 2003)

We consider a lattice of coupled circle maps, a popular model for the study of mode-locked phenomena. We find that the onset of spatiotemporal intermittency (STI) in this system is analogous to directed percolation (DP), with the transition being to a unique absorbing state for low nonlinearities, and to weakly chaotic absorbing states for high nonlinearities. We find that the complete set of static exponents and spreading exponents at all critical points match those of DP very convincingly. Further, hyperscaling relations are fulfilled, leading to independent controls and consistency checks of the values of all the critical exponents. These results provide an example in support of the conjecture that the onset of STI in deterministic models belongs to the DP universality class. Nonuniversal spreading exponents are seen only for the cases where the initial state is homogeneous with symmetrically placed seeds leading to strictly symmetric spreading. However, very small departures from homogeneity are sufficient to restore the DP exponents.

DOI: 10.1103/PhysRevE.67.056218 PACS number(s): 05.45.Ra

I. INTRODUCTION

Spatiotemporal intermittency (STI) in coupled map lattices (CML) has been extensively studied in varied contexts, especially as it is the precursor of fully developed spatiotemporal chaos in extended dynamical systems [1]. There are two types of motion seen in systems exhibiting STI: laminar and turbulent. The laminar region is characterized by periodic or even weakly chaotic dynamics, while no spatiotemporally regular structure can be seen in the turbulent regime. A laminar of ''inactive'' site becomes turbulent or ''active'' at a particular time only if at least one of its neighbors was turbulent at an earlier time, i.e., there is no spontaneous creation of turbulent sites. Hence a turbulent site can either relax spontaneously to its laminar state or contaminate its neighbors [2]. To be more precise, if the propagation rate of turbulence is below a certain threshold, the turbulent states die out and the system remains in the laminar state for all time (laminar phase or inactive phase). On the other hand, on exceeding this threshold, the turbulent states start ''percolating'' in space-time (turbulent or inactive phase). Also, once all the sites relax spontaneously to its laminar state, the system gets trapped in this state for all time. Hence, the laminar state is ''absorbing'' in STI. The existence of the absorbing states led to the conjecture by Pomeau that STI in deterministic models also belongs to the directed percolation (DP) universality class [3].

While there is substantial evidence of DP universality in stochastic models exhibiting a continuous transition to an absorbing state [4–6], it is of considerable interest to examine the robustness of DP critical behavior in systems with *completely deterministic evolution rules*. To this end, Chate and Manneville introduced a simple CML [7] exhibiting STI and possessing infinitely many absorbing states. Surprisingly, it was found that not only were the exponents governing the onset of STI different from those of DP, they were also nonuniversal in nature [7]. This nonuniversal behavior was considered to be due to the existence of traveling solitary excitations (solitons) with long lifetimes in this model. In Ref. [8] it was argued that the existence of these solitons, which spoiled the DP nature of the universality class, was a consequence of the synchronous updating rule and asynchronous updates were tried with this model. This asynchronous update destroyed the solitons and then the static exponents were found to be consistent with DP exponents [8]. Later it was also observed that even finite lifetime solitons could completely change the nature of transition in a weak soliton region [9]. This indicates that it is *nontrivial to map deterministic dynamics to stochastic behavior* as various spatiotemporal structures (such as these solitons) may introduce long range correlations, which ruin the analogy [10]. Hence, it is of considerable interest to find CMLs with regimes where there are no additional special spatiotemporal structures, which can be used as clean testbeds for checking the validity of the DP universality class.

Since the state variables of CMLs can often be identified with physical quantities (such as, voltage, current, pressure, temperature, concentration, or velocity) in fairly realistic situations, it is conceivable that such models may suggest various experimental possibilities for observing DP, which still remains an outstanding problem [4]. Further, STI is a common phenomenon of many extended systems and is seen, for instance, in experiments on convection [11] and in the ''printers instability'' [12]. Therefore, if the onset of STI does in fact exhibit DP universality, then it could lead to promising candidates for observing DP in real phenomena. A recent experiment [13] that studies the transition to STI in a one-dimensional system of ferrofluid spikes driven by an external oscillating magnetic field, finds that four of the five measured exponents are in agreement with DP exponents within experimental resolution. We note, however, that the fifth exponent shows a significant departure from DP behav-

*Email address: janaki@wagner.ucsc.edu
†Email address: sudeshna@imsc.res.in
‡Email address: gupte@chaos.iitm.ernet.in

ior, which may be due to the finite size of the apparatus or due to the absence of a true absorbing state. We also note that this is the only experimental system that shows DP exponents so far (see Table I in Ref. [13]).

In the last decade, the Chate-Manneville CML and its variants [9] have been the only class of CML studied extensively in this context. Numerical evidence from more varied sources is required, especially in the absence of analytical results, in order to settle the question of DP universality in transitions occurring in deterministic systems. Thus, it is of considerable interest to be able to find examples of this correspondence in systems quite distinct from the Chate-Manneville class, and with qualitatively different absorbing states, that would lend credence to the Pomeau conjecture. This work provides one such example.

In this paper, we consider the coupled circle map lattice [14] that has been used to model the mode-locking behavior of the type seen in coupled oscillator systems and in diverse experimental systems such as charge density waves and Josephson-Junction arrays [15]. We find that this system has regimes that show spatiotemporal intermittency, with both unique and weakly chaotic laminar regions, at different values of the nonlinearity parameter. Importantly, the solitons that spoilt the DP behavior in the earlier studies [8,9] are completely absent here. Thus, we have, at hand, a CML without any potentially problematic coherent spatiotemporal structures, showing the onset of spatiotemporal intermittency very cleanly. This CML can then serve as a good testbed for checking the validity of the DP universality class for both unique and fluctuating absorbing states.

We will now present results from this system, which strongly indicate that the complete set of static exponents characterizing the transition to STI are completely consistent with DP, both for unique and for weakly chaotic absorbing states. We will also show that the spreading exponents (dynamic exponents) for unique as well as fluctuating absorbing states agree within 3% of those obtained in DP. Further, we will demonstrate that the hyperscaling relations in case of the static as well as the spreading exponents are also satisfied. Thus we will provide two distinct examples of clean DP universality in transitions to STI, one of which constitutes an example of this correspondence in a CML with a unique absorbing state, and the other constitutes an example of this correspondence when there exists weakly chaotic absorbing state.

We also obtain spreading exponents from highly symmetric initial states where active seed(s) are symmetrically placed in a homogeneous background. Such initial states lead to strictly symmetric spreading and nonuniversal exponents. This is consistent with the comment of Grassberger *et al.* [6] that nonuniversal exponents cannot be expected for spreading from non-natural initial states. We note that very small departures from homogeneity in the initial state are sufficient to restore DP exponents.

II. STATIC (BULK) EXPONENTS

First, recall the coupled circle map lattice [16]:

$$\theta_{i,t+1}=(1-\epsilon)f(\theta_i,t)+\frac{\epsilon}{2}[f(\theta_{i-1,t})+f(\theta_{i+1,t})] \mod 1, \tag{1}$$

where t is the discrete time index, and i is the site index ($i=1,...L$), with L being the system size. Parameter ϵ gives the strength of the diffusive coupling between site i and its two neighbors. The local on-site map is given by

$$f(\theta)=\theta+\omega-\frac{k}{2\pi}\sin(2\pi\theta), \tag{2}$$

where parameter k gives the nonlinearity. This CML has been studied extensively with parallel updates and has a rich phase diagram with many types of attractors and strong sensitivity to initial conditions [16,17]. In particular, this system also has regimes of STI when evolved in parallel with random initial conditions. Figures 1 and 2 show space-time plots of the spatiotemporal intermittency observed in two different STI regimes. It is clear that no traveling wave solitonlike structures are seen in this regime. Hence, it is not necessary to introduce any asynchronicity here to destroy ''solitonic'' behavior, as this system is naturally free of such spatiotemporal excitations in the parameter region studied here.

We shall now study the onset of spatiotemporal intermittency in this system. Interestingly, as mentioned before, two qualitatively distinct absorbing regions can be found in this system.

(i) When the nonlinearity parameter $k=1$, there are regions of $(\epsilon-\omega)$ space where the system goes to the synchronized spatiotemporal fixed point $\theta^*=1/2\pi\sin^{-1}(2\pi\omega/k)$. This constitutes a *unique* absorbing state (see Fig. 1). We closely scrutinize the critical behavior at two critical points in this regime: $\omega=0.064$, $\epsilon=0.637\,75$ and $\omega=0.068$, $\epsilon=0.732\,77$. These mark the transition from a laminar phase to STI. The turbulent sites here are those which are different from θ^*.

(ii) When nonlinearity parameter $k=3.1$, there are regions of $(\epsilon-\omega)$ space where sites with any value less than $\frac{1}{2}$ con-

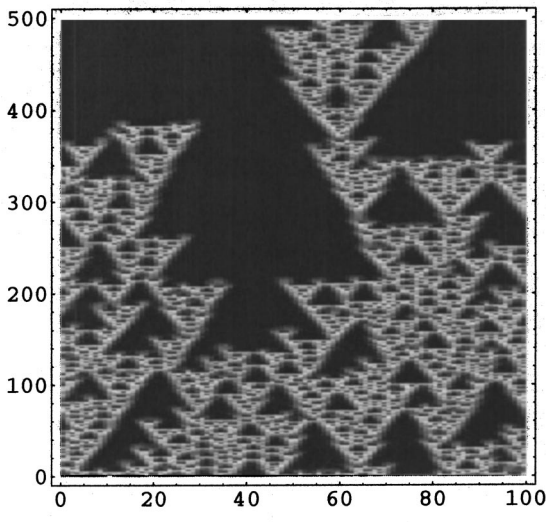

FIG. 1. STI in a synchronously updated coupled circle map lattice of size $L=100$ with parameters $k=1$, $\omega=0.068$, $\epsilon_c=0.732\,77$. The horizontal axis is the site index $i=1,...,L$ and the vertical axis is discrete time t. The absorbing region (black) has sites at the spatiotemporal fixed point of the system.

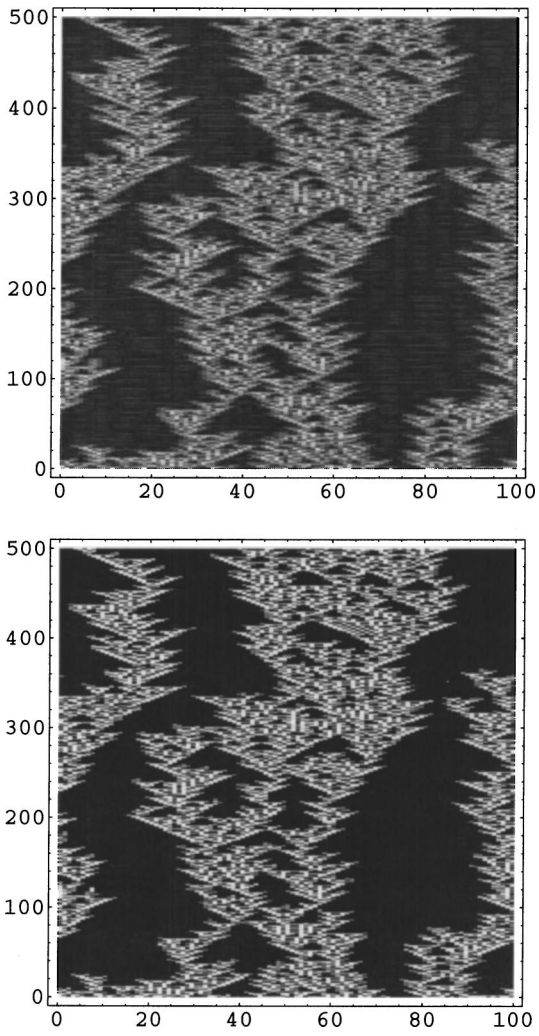

FIG. 2. STI in a synchronously updated coupled circle map lattice of size $L=100$ with parameters $k=3.1$, $\omega=0.18$, $\epsilon_c=0.701$, where the absorbing region has sites below $\frac{1}{2}$ and is not unique. The horizontal axis is the site index $i=1,...,L$ and the vertical axis is discrete time t. The top figure is obtained from a density plot of the actual θ values (the absorbing regions appear dark). The figure below is a coarse grained plot of the above (black is an absorbing site and white is an active one).

stitute the absorbing states, and sites whose values are greater than $\frac{1}{2}$ constitute the turbulent states [see Figs. 2(a) and 2(b)]. So, now the absorbing states are *infinitely many*, as also *weakly chaotic*. We study the critical behavior at two critical points in this regime: $\omega=0.18$, $\epsilon=0.701$, and $\omega=0.19$, $\epsilon=0.656\,12$.

As mentioned earlier, we initiate the evolution with random initial conditions and let the system evolve under parallel updates. The DP universality class is characterized by a set of critical exponents that describe the scaling behavior of the quantities of physical interest. The physical quantities of interest for such systems are (a) the escape time τ, which is the number of time steps elapsed before the system reaches its laminar state and (b) the order parameter $m(\epsilon,L,t)$ which is the fraction of turbulent sites in the lattice at time t. From finite-size scaling arguments, it is expected that τ depends on L such that

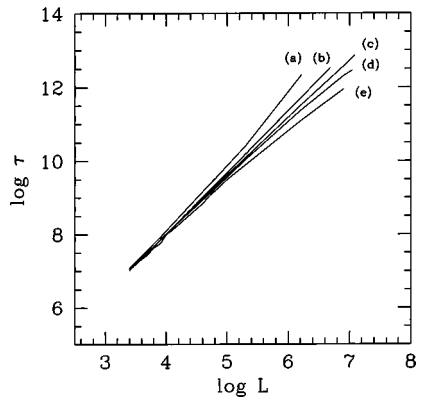

FIG. 3. Log-log plot (base e) of escape time τ vs lattice size L for parameters $k=1$, $\omega=0.068$, and (a) $\epsilon=0.639$, (b) $\epsilon=0.638$, (c) $\epsilon_c=0.63775$, (d) $\epsilon=0.637$, and (e) $\epsilon=0.635$.

$$\tau(\omega,\epsilon)=\begin{cases}\log L, & \text{laminar phase}\\ L^z, & \text{critical phase}\\ \exp L^c, & \text{turbulent phase.}\end{cases}$$

Here, c is a constant of order unity and the critical point is identified as the set of parameter values at which τ shows power-law behavior with z being the critical exponent.

We compute the above quantities for our CML averaged over an ensemble of 10^4 initial conditions. The dependence of τ on L for different values of ϵ is shown on a log-log plot in Fig. 3. Figure 3 shows this dependence at parameter values $k=1$, $\omega=0.068$ (i.e., at parameter values that correspond to a unique absorbing state). It is clear from the graph that an algebraic increase can be seen at the value $\epsilon_c=0.637\,75$. A similar analysis was carried out for parameter values $k=1$, $\omega=0.064$, where a unique absorbing state can again be seen, and gave the critical value $\epsilon_c=0.732\,77$. Weakly chaotic absorbing states were seen at parameter values $k=3.1$, $\omega=0.18$, and $\omega=0.19$. Here the critical values of parameters turned out to be $\epsilon_c=0.701\,00$ for the first case and $\epsilon_c=0.656\,12$ for the second case. The critical exponent z was estimated at these critical values for all four cases. The log-log plot of the escape time τ against the system size L is shown in Fig. 4. It is clear that the same exponent z is seen for all four cases and turns out to lie in the range 1.58–1.59, which is completely consistent with the DP value for this exponent. (See Table I.)

Figure 5 displays the dependence of the order parameter $m(\epsilon,L,t)$ on ϵ, around the critical point ϵ_c. When the critical line is approached from above, with other parameters being held fixed, the order parameter m is expected to scale as

$$m\sim(\epsilon-\epsilon_c)^{\beta},\quad \epsilon\to\epsilon_c^{+}. \tag{3}$$

Sufficiently close to the critical point, reasonable scaling over a limited range can be obtained for our system, even when approaching the critical point from below (though this is approached extremely slowly, underscoring the difficulty of accurately estimating the critical behavior of stationary states [10,18]).

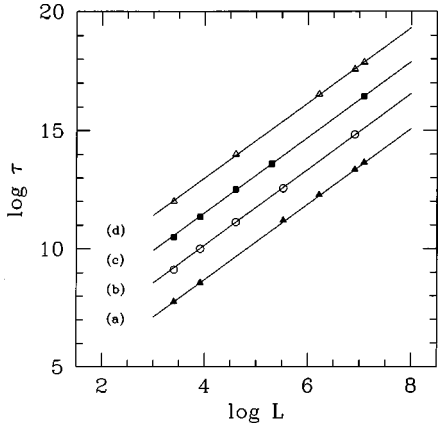

FIG. 4. Log-log plot (base e) of escape time τ vs lattice size L for all four critical points: (a) $k=1$, $\omega=0.068$, $\epsilon_c=0.637\,75$; (b) $k=1$, $\omega=0.064$, $\epsilon_c=0.732\,77$ (when there exists an unique absorbing state); (c) $k=3.1$, $\omega=0.18$, $\epsilon_c=0.701\,00$; and (d) $k=3.1$, $\omega=0.19$, $\epsilon_c=0.656\,12$ (with fluctuating absorbing states). Table I gives the exponent z of the power law fits for the different critical points.

Now for $t \ll \tau$, the order parameter is expected to obey the scaling relation

$$m(\epsilon_c, L, t) \approx t^{-\beta/\nu z}. \tag{4}$$

Therefore the log-log plots of m as a function of time t for various lattice sizes must fall on one line when $t \ll \tau$ and the power $-\beta/\nu z$ must correspond to the slope of the graph for these regimes. The order parameter is plotted as a function of t on log-log plot in Figs. 6 and 7, where the data in Fig. 6 is obtained for parameter values $k=1$, $\omega=0.068$, and $\epsilon_c=0.637\,75$ (the unique absorbing state case, and that in Fig. 7 is obtained for $k=3.1$,) $\omega=0.19$, and $\epsilon_c=0.656\,12$ (the case with weakly chaotic absorbing states). In both cases, the data for $L=50$, 100, 300, 500, 1000 collapse on to one line, the slope of which gives $-\beta/\nu z=-0.16$.

TABLE I. Critical static exponents of the synchronously updated coupled circle map lattice for four critical points. The first two critical points correspond to transitions to a unique absorbing case, while the third and fourth points correspond to weakly chaotic absorbing states. The last row shows the corresponding exponents of directed percolation.

k	ω	ϵ	z	β	ν	η'
1	0.068	0.637 75	1.580	0.28	1.10	1.49
1	0.064	0.732 77	1.591	0.28	1.10	1.50
3.1	0.18	0.701 00	1.597	0.26	1.12	1.50
3.1	0.19	0.656 12	1.591	0.28	1.10	1.49
DP			1.58	0.28	1.10	1.51

The order parameter of systems that belong to the directed percolation universality class satisfies the scaling function

$$m(\epsilon_c, L, t) \sim L^{-\beta/\nu} g_{ml}(t/L^z) \tag{5}$$

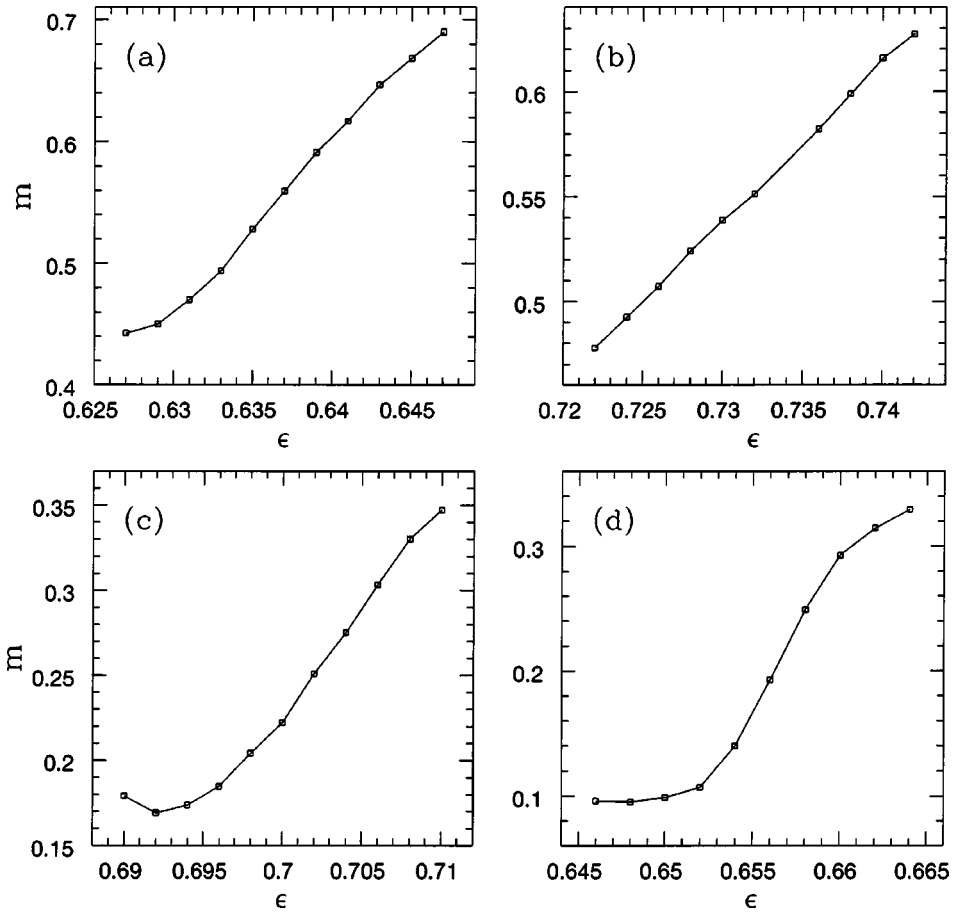

FIG. 5. Plot of order parameter m vs ϵ, around the critical point ϵ_c for the four cases: (a) $k=1$, $\omega=0.068$, $\epsilon_c=0.637\,75$; (b) $k=1$, $\omega=0.064$, $\epsilon_c=0.732\,77$; (c) $k=3.1$, $\omega=0.18$, $\epsilon_c=0.701$; and (d) $k=3.1$, $\omega=0.19$, $\epsilon_c=0.656\,12$. The order parameter m is calculated for a lattice of size $L=1000$ at time $t=5000$.

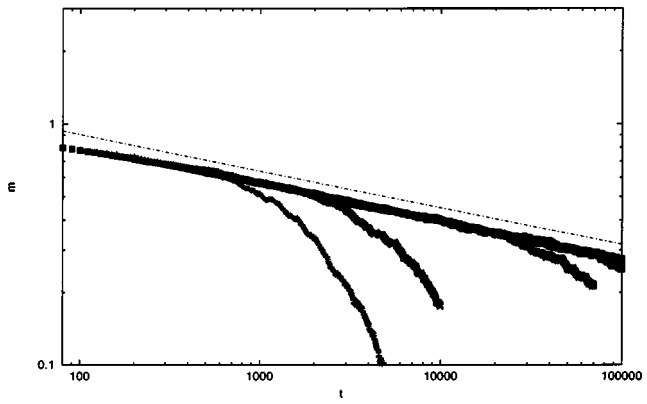

FIG. 6. Log-log (base 10) plot of order parameter $m(t)$ vs t for different lattice sizes at the critical point: $k=1$, $\omega=0.068$, and $\epsilon_c=0.637\,75$ (when there exists a unique absorbing state). For $t \ll \tau$, the data collapse for $L=50$, 100, 300, 500, 1000 onto one line, the slope of which gives $-\beta/\nu z=-0.16$

at the critical value $\epsilon=\epsilon_c$. We plot the order parameter for our CML at the critical values above in Figs. 8 and 9. The data with scaled variables $M=mL^{\beta/\nu}$ and $T=t/L^z$ fall on one curve for various lattice sizes indicating dynamical scaling (see Figs. 8 and 9, parameter values are as given in the figure captions). This further substantiates the claim that the behavior of the sine circle map CML falls in the directed percolation universality class.

The exponent ν can be extracted independently, by using the scaling relation

$$\tau(L,\delta_c) \approx \phi^z f(L/\phi), \tag{6}$$

where ϕ is the correlation length that diverges as $\phi \approx {\delta_c}^{-\nu}$ and δ_c is given by $\epsilon-\epsilon_c$ [19]. Therefore, ν can be obtained by adjusting its value till the scaled variables $L\delta_c^{\nu}$ and $\tau\delta_c^{\nu z}$ collapse onto a single curve. Thus, the exponent β can be obtained from Eq. (5).

To extract further critical exponents, we obtain the correlations from the pair correlation function given by

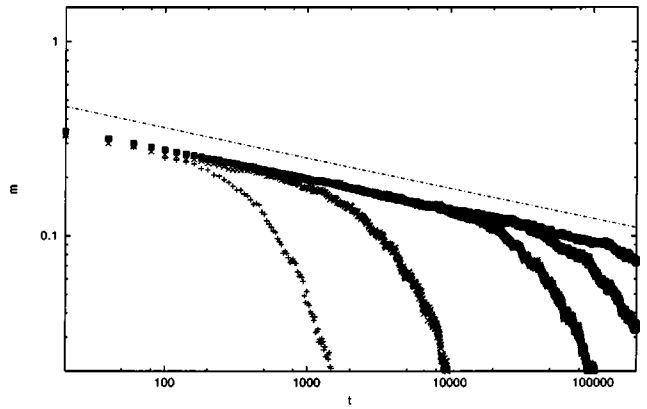

FIG. 7. Log-log (base 10) plot of order parameter $m(t)$ versus t for different lattice sizes at the critical point: $k=3.1$, $\omega=0.19$, and $\epsilon_c=0.656\,12$ (a case with weakly chaotic absorbing states). For $t \ll \tau$, the data collapse for $L=50$, 100, 300, 500, 1000 onto one line, the slope of which gives $-\beta/\nu z=-0.16$.

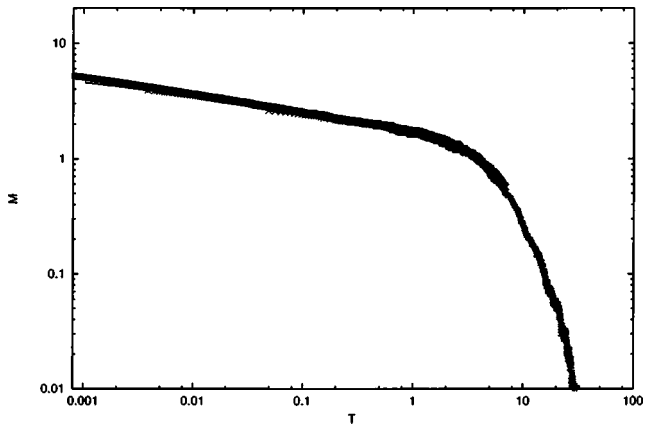

FIG. 8. Log-log (base 10) plot of $M=mL^{\beta/\nu}$ vs $T=t/L^Z$ at the critical point: $k=1$, $\omega=0.068$, and $\epsilon_c=0.637\,75$ (when there exists a unique absorbing state). This rescaling of the order parameter according to Eq. (5) yields independent estimates for β/ν and z. The data for system sizes L ranging from 2^4 to 2^{10} collapse onto one curve.

$$C_j(t)=\frac{1}{L}\sum_{i=1}^{L}\langle u_i(t)u_{i+j}(t)\rangle-\langle u_i(t)\rangle^2, \tag{7}$$

where the angular brackets denote the averaging over different initial conditions. At criticality, one expects an algebraic decay of correlation [19]:

$$C_j(t)\approx j^{1-\eta'},$$

where η' is the associated critical exponent. The log-log plot of the spatial correlation function at $k=1$, $\omega=0.064$, $\epsilon_c=0.732\,77$ can be seen in Fig. 10. The log-log plot of the correlation function approaches a straight line with slope $1-\eta'$ at large times. The value of exponent η' turns out to be ~ 1.5, which is consistent with the directed percolation value. The values of the exponent at the other critical set of param-

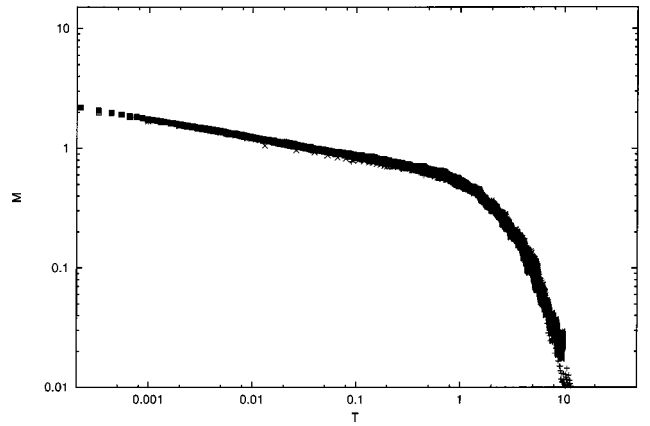

FIG. 9. Log-log (base 10) plot of $M=mL^{\beta/\nu}$ vs $T=t/L^Z$ at the critical point: $k=3.1$, $\omega=0.19$, and $\epsilon_c=0.656\,12$ (when there are weakly chaotic absorbing states). This rescaling of the order parameter according to Eq. (5) yields independent estimates for β/ν and z. The data for system sizes L ranging from 2^4 to 2^{10} collapse onto one curve.

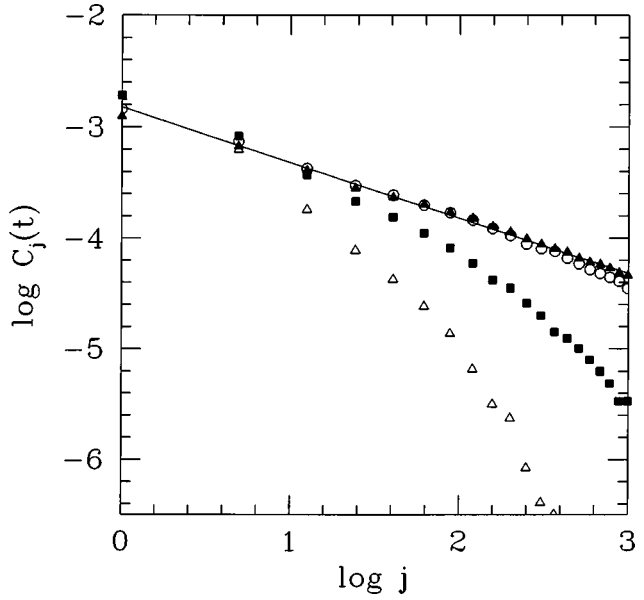

FIG. 10. Log-log plot (base e) of the spatial correlation function $C_j(t)$ vs j at various times $t(=100,300,500,1000)$ at the critical point: $k=1$, $\omega=0.064$, $\epsilon_c=0.73277$. $C_j(t)$ approaches a straight line with slope $1-\eta'$ for large times indicating an algebraic decay.

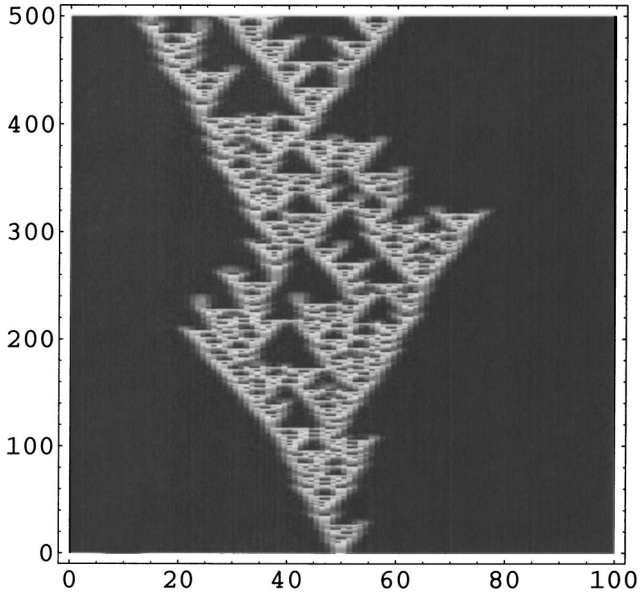

FIG. 11. Spreading of two active seeds in an otherwise absorbing lattice of size $L=100$ at critical point $k=1$, $\omega=0.068$, $\epsilon_c=0.732\,77$. The horizontal axis is the site index $i=1,...,L$ and the vertical axis is discrete time t. The absorbing region (black) is unique here, with all sites at the spatiotemporal fixed point of the system.

eter values are listed in Table I. Directed-percolation-like behavior is observed for the entire set.

Thus we have obtained the *complete set of static (bulk) exponents*, namely, z, β, ν, η', that characterize the DP class (see Table I). Clearly, the values of the exponents obtained for the coupled circle map lattice are in excellent agreement with the DP values for both unique as well as the weakly chaotic absorbing states. The exponents also satisfy the hyperscaling relation, $2\beta/\nu=d-2+\eta'$, where $d=1$.

III. SPREADING EXPONENTS

In the preceding section we obtained the static exponents, also known as the bulk exponents for our CML, and found that they were in good agreement with those of DP. We shall now compute a set of dynamical exponents, called the spreading exponents, from the temporal evolution of a nearly absorbing system with a localized disturbance, i.e., with only a few contiguous active (turbulent) sites in an otherwise absorbing state. The quantities of interest are, the time dependence of $N(t)$, the number of active sites at time t averaged over all runs, $P(t)$, the survival probability, or the fraction of initial conditions that show a nonzero number of active sites (or a propagating disturbance) at time t and $R^2(t)$, the mean squared deviation from the origin of the turbulent activity averaged over surviving runs alone. The spreading exponents are obtained from the time dependence of these quantities, which show scaling behavior at criticality. At criticality, we have

$$N(t)\approx t^{\eta}, \quad P(t)\approx t^{-\delta}, \quad R^2(t)\approx t^{z_s}.$$

Also, $\delta=\beta/\nu z$. We shall now compute these quantities for our system and compare them with those of DP.

For $k=1$, when one starts with a single active site in an otherwise absorbing lattice with all other sites at θ^*, the symmetric diffusive coupling will yield *strictly* symmetric temporal spreading about the single active site. Further, we find that the system goes to its absorbing state in about ten time steps of evolution. Hence, a meaningful scaling cannot be obtained here. However, using a larger number of active

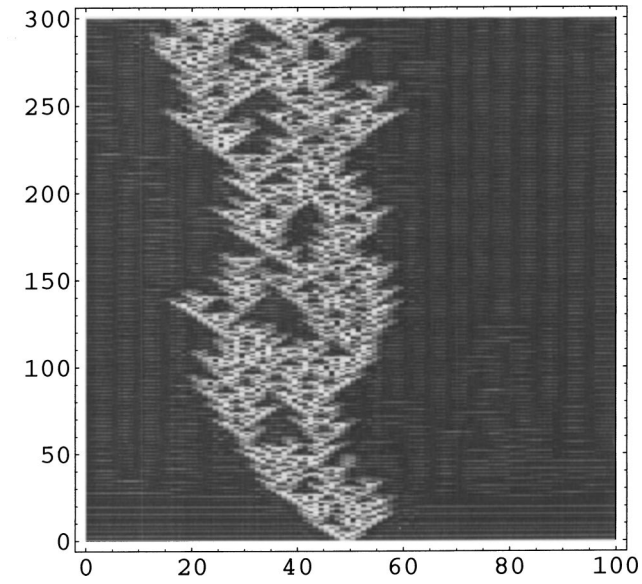

FIG. 12. Spreading of two active seeds in an otherwise absorbing lattice of size $L=100$ at critical point $k=3.1$, $\omega=0.18$, $\epsilon_c=0.701$. The horizontal axis is the site index $i=1,...,L$ and the vertical axis is discrete time t. The absorbing region (dark) has all sites below $\frac{1}{2}$ and is not unique.

TABLE II. Spreading exponents of the synchronously updated coupled circle map lattice for four critical points. Two active seeds in an absorbing configuration are used as the initial condition. For the first two critical points there exists a unique absorbing state, while for the third and fourth points one can have many different absorbing states and consequently many different initial absorbing backgrounds. However, we notice that the exponents obtained are quite the same for different initial preparations and thus appear universal for two active seeds. The last row shows the corresponding exponents of directed percolation.

k	ω	ϵ	η	δ	z_s
1	0.068	0.637 75	0.292	0.153	1.243
1	0.064	0.732 77	0.302	0.158	1.259
3.1	0.18	0.701 00	0.310	0.157	1.272
3.1	0.19	0.656 12	0.308	0.156	1.251
DP			0.313	0.159	1.26

sites, placed symmetrically about the spreading center increases the scaling range considerably and gives better statistics. We find that the spreading exponents thus obtained are strongly dependent on the initial number of active sites, as well as on the actual initial values of the active seeds. For instance, in a lattice of size 1000, spreading from 200 equal active seeds yields the spreading exponent $\eta \sim 0.21$, while if one starts with ten equal active seeds in the same lattice, η is close to 0.0. Thus, the spreading exponents from strictly symmetric spreading are nonuniversal.

To counter the strictly symmetric spreading, we need two or more contiguous random active sites (see Fig. 11) in the background fixed at θ^*. We find that the full set of spreading exponents obtained via the expressions above, starting with two or more random active seeds (see Figs. 13–15) agree within 3% of the DP values (see Table II). This indicates that universal power laws exist for the case of asymmetric spreading in an absorbing background.

For $k=3.1$ there is no unique absorbing configuration as above, and any initial configuration with values less than $\frac{1}{2}$ constitutes an absorbing background. We find that we can now obtain reasonable asymmetric spreading (and consequently the exponents) with just a single active seed and these exponents are the same as those obtained from spreading from two or three contiguous active sites (see Fig. 12). Again the complete set of spreading exponents agree with those of DP within 3% at all critical points (see Table II and Figs. 13–15).

Note, however, that even at $k=3.1$, if we start with the very special initial background of all sites at some fixed θ_{bg}, then naturally a single active seed will again spread strictly symmetrically. The exponent obtained from this symmetric spreading is nonuniversal and varies with θ_{bg}. For instance, if $\theta_{bg}=0.4$, the spreading exponent $\eta=0.07$; while, if $\theta_{bg}=0.0$, $\eta=0.05$. According to Ref. [6] one should not expect universal scaling laws for spreading from non-natural initial states. The nonuniversality of the spreading exponents we observe here lends credence to this idea and indicates that there are no universal power laws when the background is homogeneous (which is non-natural in this parameter regime). However, even a slight breaking of the homogeneity

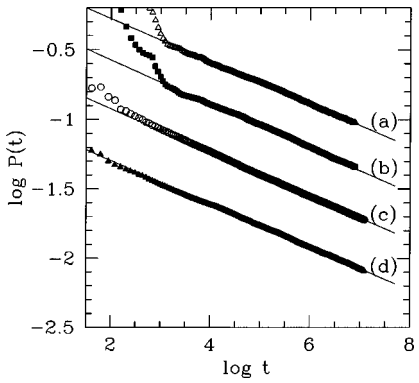

FIG. 14. Log-log plot (base e) of $P(t)$ vs t for all four critical points: (a) $k=1$, $\omega=0.068$, $\epsilon_c=0.637\,75$; (b) $k=1$, $\omega=0.064$, $\epsilon_c=0.732\,77$; (c) $k=3.1$, $\omega=0.18$, $\epsilon_c=0.701\,00$; and (d) $k=3.1$, $\omega=0.19$, $\epsilon_c=0.656\,12$. Table II gives the exponent δ of the power law fits for the different critical points.

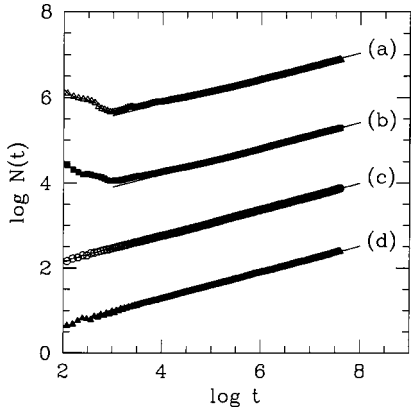

FIG. 13. Log-log plot (base e) of $N(t)$ vs t for all four critical points: (a) $k=1$, $\omega=0.068$, $\epsilon_c=0.637\,75$; (b) $k=1$, $\omega=0.064$, $\epsilon_c=0.732\,77$; (c) $k=3.1$, $\omega=0.18$, $\epsilon_c=0.701\,00$; and (d) $k=3.1$, $\omega=0.19$, $\epsilon_c=0.656\,12$. Table II gives the exponent η of the power law fits for the different critical points.

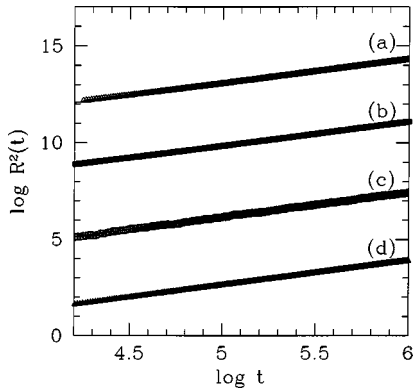

FIG. 15. Log-log plot (base e) of $R^2(t)$ vs t for all four critical points: (a) $k=1$, $\omega=0.068$, $\epsilon_c=0.637\,75$; (b) $k=1$, $\omega=0.064$, $\epsilon_c=0.732\,77$; (c) $k=3.1$, $\omega=0.18$, $\epsilon_c=0.701\,00$; and (d) $k=3.1$, $\omega=0.19$, $\epsilon_c=0.656\,12$. Table II gives the exponent z_s of the power law fits for the different critical points.

of the background, by the introduction of a very small spread around θ_{bg} ($\sim 10^{-4}$), restores the DP universality.

IV. CONCLUSIONS

The evaluation of the complete set of static and spreading exponents at the onset of spatiotemporal intermittency in coupled circle map lattices shows that this transition clearly falls in the universality class of directed percolation. All the critical characteristics of directed percolation, such as hyperscaling, are fulfilled, leading to independent controls and consistency checks of the values of all the critical exponents. DP exponents are seen at low values of nonlinearity for a unique absorbing state and at high values of nonlinearity for weakly chaotic absorbing states. It is not necessary to introduce asynchronicity or an extra dimension to tune out solitonic behavior since no solitonic behavior is seen in this model. Thus this model constitutes a clean system where DP exponents are very naturally seen. Nonuniversal spreading exponents can be observed in the case of strictly symmetric spreads obtained from active seeds placed symmetrically in homogeneous backgrounds, but DP exponents are restored if the strict symmetry of the spread is broken by slight departures from either the uniformity of the background or the symmetry of active seeds. Model studies such as these, showing the clean correspondence between the onset of STI and directed percolation, could then lead to promising new candidates for observing DP in real phenomena.

[1] *Theory and Applications of Coupled Map Lattices*, edited by K. Kaneko (Wiley, New York, 1993), and references therein. Specifically, the critical scaling behavior of CMLs has been investigated in papers such as: J. M. Houlrik *et al.*, Phys. Rev. A **41**, 4210 (1990); O. Moriyama and M. Matsushita, J. Phys. Soc. Jpn. **65**, 3478 (1996).

[2] This type of STI is known as the type-I STI in the literature.

[3] Y. Pomeau, Physica D **23**, 3 (1986).

[4] P. Grassberger, Z. Phys. B: Condens. Matter **47**, 365 (1982); H. Hinrichsen, e-print cond-mat/0001070, and references therein.

[5] I. Jensen, J. Phys. A **29**, 7013 (1996); I. Jensen and R. Dickman, Phys. Rev. E **48**, 1710 (1993); J. F. F. Mendes *et al.*, J. Phys. A **27**, 3019 (1994); M. A. Munoz *et al.*, J. Stat. Phys. **91**, 541 (1998); Phys. Rev. E **56**, 5101 (1997).

[6] P. Grassberger *et al.*, Phys. Rev. E **55**, 2488 (1997).

[7] H. Chate and P. Manneville, Physica D **32**, 409 (1988).

[8] J. Rolf, T. Bohr, and M. H. Jensen, Phys. Rev. E **57**, R2503 (1998).

[9] T. Bohr *et al.*, Phys. Rev. Lett. **86**, 5482 (2001).

[10] P. Grassberger and T. Schreiber, Physica D **50**, 177 (1991).

[11] S. Ciliberto and P. Bigazzi, Phys. Rev. Lett. **60**, 286 (1988); F. Daviaud, M. Dubois, and P. Berge, Europhys. Lett. **9**, 441 (1989).

[12] M. Rabaud, S. Michalland, and Y. Couder, Phys. Rev. Lett. **64**, 184 (1990); S. Michalland and M. Rabaud, Physica D **61**, 197 (1992).

[13] P. Rupp, R. Richter, and I. Rehberg, e-print cond-mat/0201308.

[14] N. Chatterjee and N. Gupte, Phys. Rev. E **53**, 4457 (1996).

[15] P. Bak *et al.*, Solid State Commun. **51**, 231 (1984); K. Wiesenfeld and P. Hadley, Phys. Rev. Lett. **62**, 1335 (1989).

[16] G. R. Pradhan, N. Chatterjee, and N. Gupte, Phys. Rev. E **65**, 046227 (2002).

[17] G. R. Pradhan and N. Gupte, Int. J. Bifurcation Chaos Appl. Sci. Eng. **11**, 2501 (2001).

[18] Some nonmonotonic structure is seen in the dependence of m on ϵ for $\epsilon < \epsilon_c$ for both values of k beyond the range in the displayed figures. However, the departures from monotonicity are much milder than those seen in Ref. [10].

[19] J. M. Houlrik and M. H. Jensen, Phys. Lett. A **163**, 275 (1992).